Stem Cell Reviews and Reports
https://doi.org/10.1007/s12015-021-10227-6

Rat Adipose-Derived Stromal Cells (ADSCs) Increases the Glioblastoma Growth and Decreases the Animal Survival

Isabele Cristiana Iser[1] · Liziane Raquel Beckenkamp[1] · Juliana Hofstatter Azambuja[1] · Francine Luciano Rahmeier[2] · Paula Andreghetto Bracco[3] · Ana Paula Santin Bertoni[1] · Rita de Cássia Sant'Anna Alves[4] · Elizandra Braganhol[1] · Léder Leal Xavier[5] · Marilda da Cruz Fernandes[2] · Guido Lenz[6] · Márcia Rosângela Wink[1]

Accepted: 25 July 2021

Abstract
Many studies have shown that mesenchymal stromal cells (MSCs) and their secreted factors may modulate the biology of tumor cells. However, how these interactions happen in vivo remains unclear. In the present study, we investigated the effects of rat adipose-derived stromal cells (ADSCs) and their conditioned medium (ADSC-CM) in glioma tumor growth and malignancy in vivo. Our results showed that when we co-injected C6 cells plus ADSCs into the rat brains, the tumors generated were larger and the animals exhibited shorter survival, when compared with tumors of the animals that received only C6 cells or C6 cells pre-treated with ADSC-CM. We further showed that the animals that received C6 plus ADSC did not present enhanced expression of CD73 (a gene highly expressed in ADSCs), indicating that the tumor volume observed in these animals was not a mere consequence of the higher density of cells administered in this group. Finally, we showed that the animals that received C6 + ADSC presented tumors with larger necrosis areas and greater infiltration of immune cells. These results indicate that the immunoregulatory properties of ADSCs and its contribution to tumor stroma can support tumor growth leading to larger zones of necrosis, recruitment of immune cells, thus facilitating tumor progression. Our data provide new insights into the way by which ADSCs and tumor cells interact and highlight the importance of understanding the fate and roles of MSCs in tumor sites in vivo, as well as their intricate crosstalk with cancer cells.

Keywords Rat adipose-derived stromal cell (ADSC) · Conditioned medium · C6 glioma cell · Tumor microenvironment · Astrocytes · Orthotopic glioma model in rat

Introduction

Glioblastoma multiforme (GBM) is the most common and lethal of the primary central nervous system tumors. Despite many advances, the mean survival time has not significantly improved and to date, there are no efficient therapeutics available for GBM. Surgical removal of the tumor, radiotherapy, and chemotherapy improve survival for a short period after which the tumor relapses, mainly because of their highly proliferative and infiltrative nature, making the

✉ Márcia Rosângela Wink
mwink@ufcspa.edu.br; marciawink@yahoo.com.br

[1] Departamento de Ciências Básicas da Saúde e Laboratório de Biologia Celular, Universidade Federal de Ciências da Saúde de Porto Alegre - UFCSPA, Rua Sarmento Leite, 245, Porto Alegre, RS CEP 90050-170, Brazil

[2] Departamento de Ciências Básicas da Saúde e Laboratório de Pesquisa em Patologia, Universidade Federal de Ciências da Saúde de Porto Alegre - UFCSPA, Porto Alegre, RS, Brazil

[3] Departamento de Estatística E Programa de Pós-Graduação Em Epidemiologia, Universidade Federal do Rio Grande do Sul – UFRGS, Porto Alegre, RS, Brazil

[4] Departamento de Patologia E Medicina Legal, Universidade Federal de Ciências da Saúde de Porto Alegre - UFCSPA, Porto Alegre, RS, Brazil

[5] Escola de Ciências da Saúde E da Vida, Pontifícia Universidade Católica do Rio Grande do Sul – PUCRS, Porto Alegre, RS, Brazil

[6] Departamento de Biofísica E Centro de Biotecnologia, Universidade Federal Do Rio Grande Do Sul - UFRGS, Porto Alegre, RS, Brazil

Published online: 17 August 2021

total resection practically impossible [1, 2]. Therefore, in recent years many efforts have been made to find new effective therapeutic tools to treat GBM.

Adipose-derived stromal cells (ADSCs) are a promising type of mesenchymal stromal cell (MSC) that are investigated for tissue and cell engineering applications. These cells are abundant and easy to obtain from adipose tissue, enhancing its potential for therapeutic purposes [3, 4]. In addition, ADSCs have been recognized for their ability to migrate to injury sites, including tumors. Their tropism for brain tumors can be used for delivering therapeutic molecules, such as genes, proteins, peptides, or small chemical molecules to the tumor site [5–7].

For a long time, it was thought that tumors were self-sufficient and independent. However, recent reports have demonstrated that tumors consist, not only of the malignant cancer cells, but also of stromal cells that are mobilized from systemic circulation and integrated into the tumor to support their microenvironment. The stroma mainly consists of myofibroblasts, tumor-associated fibroblasts (TAFs), mesenchymal stromal cells (MSCs), immune cells, endothelial cells, smooth muscle cells, as well as, non-cellular components, such as the extracellular matrix (ECM) and secreted extracellular molecules that provide support to the tumor development [8, 9].

MSCs, by themselves, are not malignant cells and function to preserve normal tissue structure and function. However, it is known that tumor cells can "corrupt" or "educate" the stromal cells present in the tumor microenvironment, enabling them to support tumor growth [10].

Previous studies have produced controversial results regarding the roles of MSCs in tumor stroma. Some studies have demonstrated that MSCs can inhibit tumor progression [11–13], whereas other investigations have revealed that MSCs promote tumor progression [14–17]. These conflicting observations may be related in part to the diversity of experimental parameters among different investigations, primary tumor origin, location, type of cells, animal model, origin of MSCs, propagation and administration of cells that can vary greatly among experiments and must be recognized [18, 19].

In our previous reports, we showed that conditioned medium (CM) from human ADSCs did not alter cancer stem cell-related features of U87 glioma cells, neither proliferation rate nor response to temozolomide (TMZ). However the CM secretome increased the migration of glioblastoma cells [20] and disrupted autophagy [20]. Thus, we further investigated the effect of CM from rat ADSC and showed that it was able to induce an EMT-like process in C6 glioma cell line, in vitro. The treatment with CM was marked by an enhanced migration capacity and increased expression of vimentin, MMP2 and NRAS. CM also promoted a reduction in adhesion and changes in cell morphology, while did not interfere in cell proliferation and cell cycle progression [21]. In this study, we aimed to investigate the effect of treatment of tumor cells with ADSC conditioned medium (ADSC-CM) on the development of glioma tumor in a rat model, as well as the effect of direct co-injection of C6 cells and ADSCs.

Materials and Methods

Cell Culture

The C6 rat glioma cell line from ATCC, was kindly provided by Dra. Ana Maria Oliveira Battastini (UFRGS, Brazil). Cells at 5–20 passages were grown in culture flasks and maintained in Dulbecco's modified Eagle's medium (DMEM) (pH 7.4) containing 1% DMEM low glucose (Sigma, St. Louis, M.O., USA), 8.4 mM HEPES, 23.8 mM $NaHCO_3$, 0.1% amphotericin B, penicillin (100 U/mL)/streptomycin (100 mg/mL) (Gibco BRL, Grand Island, NY, USA) and supplemented with 10% (v/v) fetal bovine serum (FBS) (Cultilab, São Paulo, SP, Brazil). Cells were kept at 37 °C, a minimum relative humidity of 95% and an atmosphere of 5% CO_2 in air.

Primary astrocyte cultures were prepared as previously described [22]. The cells were plated at a density of 1.5×10^5 cells/cm^2 into culture flasks pre-treated with poly-L-lysine and maintained in the same culture medium described above. Cultures were allowed to grow to confluence and used at 21–28 days. Medium was changed every 3–4 days.

ADSCs were extracted from visceral adipose tissue of *Wistar* rats (6–8 weeks), as previously described [23]. Briefly, the abdominal fat tissue from rats was first washed with phosphate-buffered saline (PBS) and dissociated mechanically with a pipette. Then, fat fragments were incubated at 37 °C for 30 min in a tube containing 2 mg/mL of collagenase Type I. After collagenase digestion, the supernatant was centrifuged at 1000 rpm and cells were resuspended in complete medium and seeded in six-well dishes. ADSCs cultures were grown in culture flasks and maintained in DMEM as described above.

All cell cultures were kept at 37 °C, a minimum relative humidity of 95% and an atmosphere of 5% CO_2 in air.

Immunophenotyping

The cultures of ADSCs were characterized to confirm the presence or absence of MSC surface markers using flow cytometry. Cells were labeled with phycoerythrin (PE)- or peridinin-chlorophyll protein (PerCP-Cy5.5)-conjugated antibodies anti-rat CD45, CD29 (Integrin beta1 chain) or CD90.2 (glycosylphosphatidylinositol-anchored glycoprotein) (Life Technologies, Carlsbad, CA, USA). The

unconjugated antibody CD11b (Life Technologies, Carlsbad, CA, USA) was incubated with FITC-conjugated anti-mouse secondary antibody (Sigma-Aldrich, St. Louis, MO, USA). Cells were analyzed using a FACS-Calibur cytometer equipped with 488 nm argon laser (Becton Dickinson, San Diego, CA, USA) with the CellQuest software. At least 10,000 events were collected. Gating was set using unstained cells.

Conditioned Medium

For all experiments, ADSC cells between the 4th and 10th passages were seeded in T75 tissue culture flask in DMEM with 10% (v/v) FBS low glucose, containing 8.4 mM HEPES (pH 7.4), 23.8 mM $NaHCO_3$, 0.1% amphotericin B, penicillin (100 U/mL)/streptomycin (100 mg/mL) (Gibco BRL, Grand Island, NY, USA) at a density of 3320 cells/cm^2. Twenty-four hours after seeding, the medium was replaced by a fresh medium and conditioned for 48 h (CM48). CM from flasks was harvested, filtrated on 0.22 µm filters (Millipore), and stored at − 80 ºC until use.

Glioma implantation

Rat C6 glioma cells at around 80% confluence were trypsinized (0.25% trypsin/EDTA solution), washed once in DMEM without FBS, spun down and resuspended in the same medium. A total of 7.5×10^5 cells in a volume of 3 µL were injected using a 10 µL Hamilton microsyringe at a depth of 6.0 mm into the right striatum (coordinates with regard to bregma: 0.5 mm posterior and 3.0 mm lateral) of adult Wistar male rats (8 weeks old, 220–260 g) anesthetized by intraperitoneal (i.p.) administration of ketamine/xylazine [24]. The protocols used in this study were approved by the Ethics Committee on Animal Use (CEUA) of Universidade Federal de Ciências da Saúde de Porto Alegre (UFCSPA), under the number 104/11, following the resolutions of the CONCEA (Conselho Nacional de Controle de Experimentação Animal). The NIH ''Guide for the Care and Use of Laboratory Animals'' (NIH publication No. 80–23, revised 1996) was followed in all experiments. The surgeries were performed with all efforts to minimize the animals suffering.

Treatment of Animals

The animals were divided into three groups as follows: (1) received 7.5×10^5 C6 cells (C6 control group), (2) received 7.5×10^5 C6 cells treated with CM48 (C6 + ADSC-CM group) and (3) received 7.5×10^5 C6 cells plus 7.5×10^5 ADSCs (C6 + ADSC group) (Fig. 1a). An additional group (4) formed by animals that received 7.5×10^5 C6 cells plus 7.5×10^5 astrocytes (C6 + astrocyte group) was added, only as a control of tumor volume and survival curve. At least seven rats per group were used for the immunohistochemical study and at least three rats for the RNA extraction.

The weight of animals was measured on day 0 and 15 days after the implant of cells and the gain of weight of the experimental groups was compared to the control group (Fig. 1b). After 20 days of the implant of cells, the perfusion was conducted. Animals were deeply anesthetized with ketamine (90 mg/kg) and xylazine (15 mg/kg) (i.p.) and injected with 1 mL heparin (Cristalia, Brazil). Using a peristaltic pump (50 mL/min), the animals were perfused through the left cardiac ventricle with 200 mL of saline solution followed by 200 mL of fixative solution of 4% paraformaldehyde diluted in 0.1 M phosphate buffer (PBS), pH 7.4. Brains were dissected from the skull, post-fixed in paraformaldehyde (4%) followed by 70% ethanol at room temperature until it was embedded in paraffin.

Pathological Analysis and Tumor Volume Quantification

At least three Hematoxylin and Eosin (H&E) Sects. (4 µm thick, paraffin embedded) from each animal were analyzed by a pathologist, blinded for the experimental data. For tumor size quantification, images were captured using an Opton camera connected to a microscope (Olympus BX 50) and the tumor area (mm^2) was determined using Image J software (National Institute of Health, Bethesda, MA). The total volume (mm^3) of the tumor was computed by the multiplication of the slice sections and by summing the segmented areas [25].

Immunohistochemical Staining

Paraffin embedded, 4 µm formalin fixed tissue sections were deparaffinized and hydrated. Endogenous peroxidase was inhibited by 5% H_2O_2 in methanol. Incubation with the following antibodies was performed overnight at 4 °C temperature: anti-glial fibrillary acidic protein (GFAP; MS-280-P0, Thermo Scientific) (1:50), anti-Ki67 (ab66155, Abcam) (1:200), anti-CD73 (D7F9A, Cell Signaling) (1:400) and CD45 (NB100-65,000, Novus) (1:50) followed by incubation with universal immuno-peroxidase polymer for rat tissue sections (Histofine Simple Stain Rat Max-PO—Nichirei Co., Tokyo, Japan). The immune complexes were visualized by using diaminobenzidine (DAB; EnVision kit; DAKO, Carpinteria, CA), according to the manufacturer's specifications. The Ki67, CD73 and CD45 immunostained sections were then counterstained with hematoxylin.

Quantitative evaluation of immunostaining

Global immunoreactivity for CD73 and CD45 was classified by a semi-quantitative score for intensity of staining,

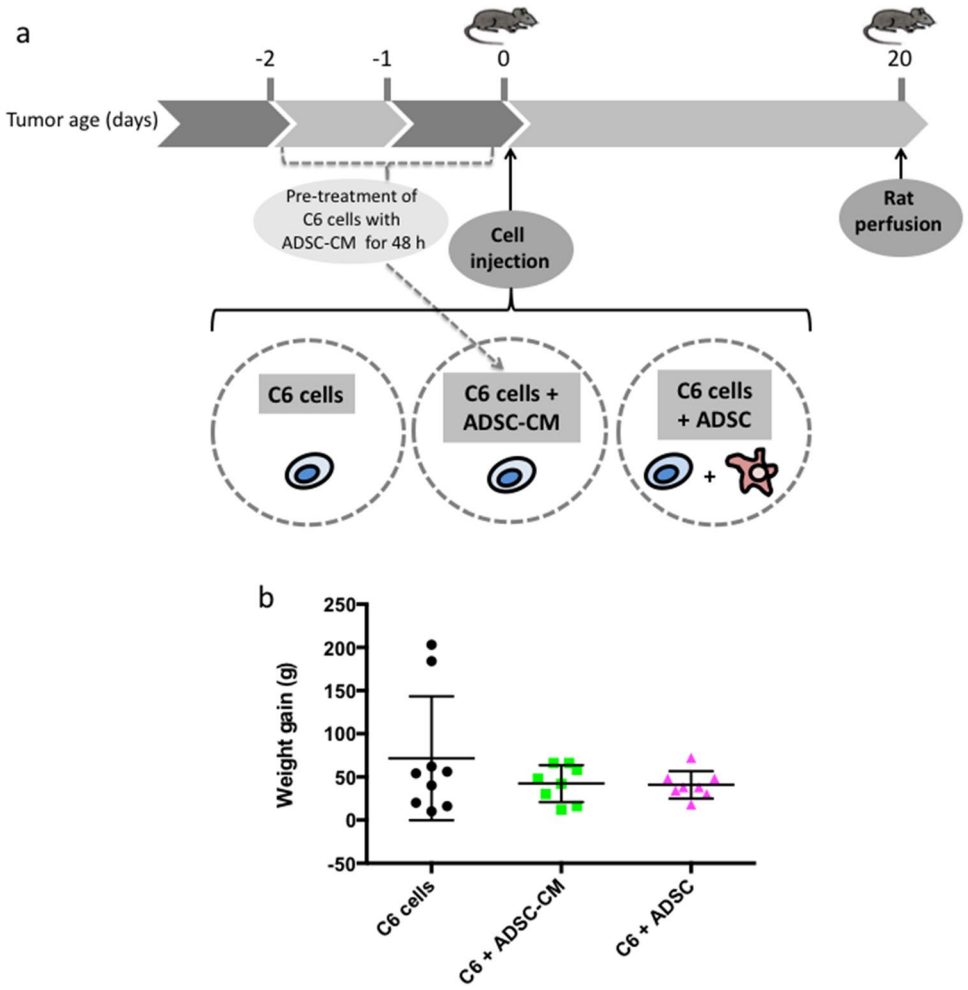

Fig. 1 Experimental design and timeline. **a** At day 0, the animals were injected with untreated C6 cells, ADSC-CM-treated C6 cells (C6 glioma cells were previously treated with ADSC-CM for 48 h), untreated C6 cells mixed at 1:1 ratio with ADSCs into the right striatum of brain of rats by stereotaxic surgery. At day 20, the animals were perfused for histological analysis. The animals whose brains were used to molecular analysis were not perfused. The animals used in the survival experiments were followed up for 90 days until euthanasia. **b** The weight gain of animals was measured at the end of 15 days after the implant of cells. The values were represented as means ± S.E.M of at least seven animals per group. Data were analyzed by ANOVA followed by post-hoc comparisons (Tukey's test). *$p < 0.05$ and **$p < 0.01$

as follows: 1 + (weak intensity), 2 + (moderate intensity), or 3 + (high intensity).

For Ki67 immunoreactivity evaluation analysis, nine digitized images (×200) from tumor bulk were obtained from each animal using an Opton camera connected to a microscope (Olympus BX 50). One randomized area of interest (AOI) measuring 5624 μm^2 was overlaid on each image. Data of glioma cell proliferation were presented by counting the percentage of Ki67 positive glioma cell nuclei.

The intensity of GFAP immunoreactivity was measured using semi-quantitative desitometric analysis [26], using an Olympus BX 50 microscope coupled to an Opton camera and Image Pro Plus software (Image Pro-plus 6.1, Media Cybernetics, Silver Spring, USA). For this analysis, three digitized images (×50) from tumor bulk, tumor edge and contralateral hemisphere (negative control). were obtained from each animal. One randomized area of interest (AOIs), measuring 15,300 μm^2 was overlaid on each image and used to estimate the regional optical density (OD).

The OD was calculated using the following formula:

$$OD(x,y) = -\log\left[(INT(x,y) - BL)/(INC - BL)\right]$$

where "OD (x,y)" is the optical density at pixel (x,y), "INT (x,y)" or intensity is the intensity at pixel (x,y), "BL" or black is the intensity generated when no light passes through the material, and "INC" is the intensity of the incidental light, which is completely white.

RT-qPCR Analysis

After 20 days of the implant of cells, at least three rats per group were decapitated, the whole brain was removed, and the tumor area was isolated. Briefly, rat glioma samples were removed and immediately preserved in RNAlater (Sigma-Aldrich Ltd.) and frozen at − 80 °C (for RNA extraction).

Total RNA from glioma cell cultures were isolated with Trizol LS reagent (Life Technologies, Carlsbad, CA, USA) in accordance with the manufacturer's instructions and stored at – 80 ºC. The cDNA was synthesized with M-MLV Reverse Transcriptase enzyme (Promega, Madison, Wis., USA) and 3 µg total RNA in a final volume of 20 µL with

a random hexamer primer in accordance with the manufacturer's instructions. Real-time PCR were carried out in an Applied-Biosystem StepOnePlus™ Real-Time PCR cycler and done in duplicate. Reaction settings were composed of an initial enzyme activation step of 20 s at 95 °C, followed by 40 cycles of 3 s at 95 °C and 30 s at 60 °C for data acquisition. Reactions were prepared in a 12.5 µL final volume composed of 6.25 µL of Fast SYBR green master mix (Applied Biosystems, Foster City, CA, USA), 0.40 µL of 10 µM primer pairs (Supplementary Table 1), 3.85 µL of water and 2µL of 1:10 diluted cDNA. Normal brain was used as a negative control. After an appropriate selection using relative standard curve method, TATA-box binding protein (TBP) was chosen as the most stable reference gene between five gene candidates and was used as a control for cDNA synthesis (data not shown). The data were presented as the ratio of genes/TBP.

Animal Survival

For survival study, the rats were treated in the same way as above and observed for 90 days after glioma implantation. After 90 days, the rats that remained alive were euthanized and the entire brain was removed and processed as described above. Survival curves were constructed by using the Kaplan–Meier method.

Statistics

All data were expressed as mean ± SEM and they were analyzed using ANOVA followed by Tukey's test for multiple comparisons of at least three independent experiments. Differences with $p < 0.05$ were considered significant. Analyses of the data were performed using GraphPad Prism version 6.0 software (GraphPad, La Jolla, CA, USA). Log-rank test (p-value < 0.05) was used to assess the survival difference between the four treatment groups and the difference between each paired group. All Survival analysis were carried out using SAS Studio through SAS OnDemand for Academics (SAS Institute, Cary, NC).

Results

ADSCs Characterization

Phenotypically, ADSCs were characterized by being negative for expression of the CD11b and CD45, hematopoietic surface markers. Flow cytometric analysis also demonstrates that cultured MSCs were positive for CD90 and CD29, as expected (Supplementary Fig. 1). As reported previously by our group, ADSCs exhibited a spindle-shaped morphology in culture and were able to differentiate into adipocytes, chondrocytes and osteoblasts [21]. These results were consistent with previous reports and indicated that the established cell line indeed consisted of ADSCs [25].

Histopathological Characterization of Glioma Model and CD73 Immunohistochemistry Analysis

C6 glioma cells are commonly used as a glioma model in studies in vitro as well as in vivo [25, 27–29]. Magnetic resonance imaging studies performed in vivo showed that the similarity of C6 gliomas to human malignant gliomas is better than other models [30]. Recently, the immune heterogeneity in rat C6 gliomas and kinetics of immune cell infiltration were analyzed. Characteristics of immune infiltrates, gene expression profiles and histopathological similarities of C6 gliomas to human GBMs samples showed that the rat C6 gliomas have similar immune immunosuppressive profile as human GBMs [31]. Therefore, we chose the orthotopic C6 glioma model as study design to investigate the role of the ADSCs in the tumor microenvironment, as the most appropriate to recapitulate features present in human GBM samples. In order to monitor the health conditions of the animals from different groups, the rats were weighed on day 0 and day 15, after implantation of cells. Although the gain of weight of the animals in the groups did not present statistical differences, there was a tendency of the animals in the C6+ADSC group to present a lower weight gain in comparison to the other groups (Fig. 1b).

Twenty days after the surgery of cells graft, the animals were euthanized and a representative figure of H&E analysis showed that mitotic index, coagulative necrosis and vascular proliferation were observed in all groups. In addition, pathological analysis identified palisading cells delineating the foci of necrosis and lymphocytic infiltration, with formation of peritumoral edema and neovascularization in all groups (Fig. 2a (panel A–I) and Supplementary Table 2). It was possible to observe that necrosis, lymphocytic infiltration and pseudopalisading were more prevalent in the C6+ADSC group, when compared to the other two groups (Supplementary Table 2). In order to estimate the fraction of ADSC that still remains in the tumor mass, 20 days after cell implantation and to analyze whether the increased cell density, or the presence of ADSCs could be contributing to the larger tumor volume of animals from the C6+ADSC group, we performed immunohistochemistry to assess the expression of CD73, a well-known marker of MSCs. The immunohistochemistry slides analyzed by a pathologist showed that the animals that received C6 plus ADSC presented a similar CD73 staining, in comparison to animals of the other two groups (Fig. 2b). This finding was very important to prove that the greater tumor volume observed in this group was not merely due to the presence of ADSCs. The fresh tumor analysis revealed that animals of group 3

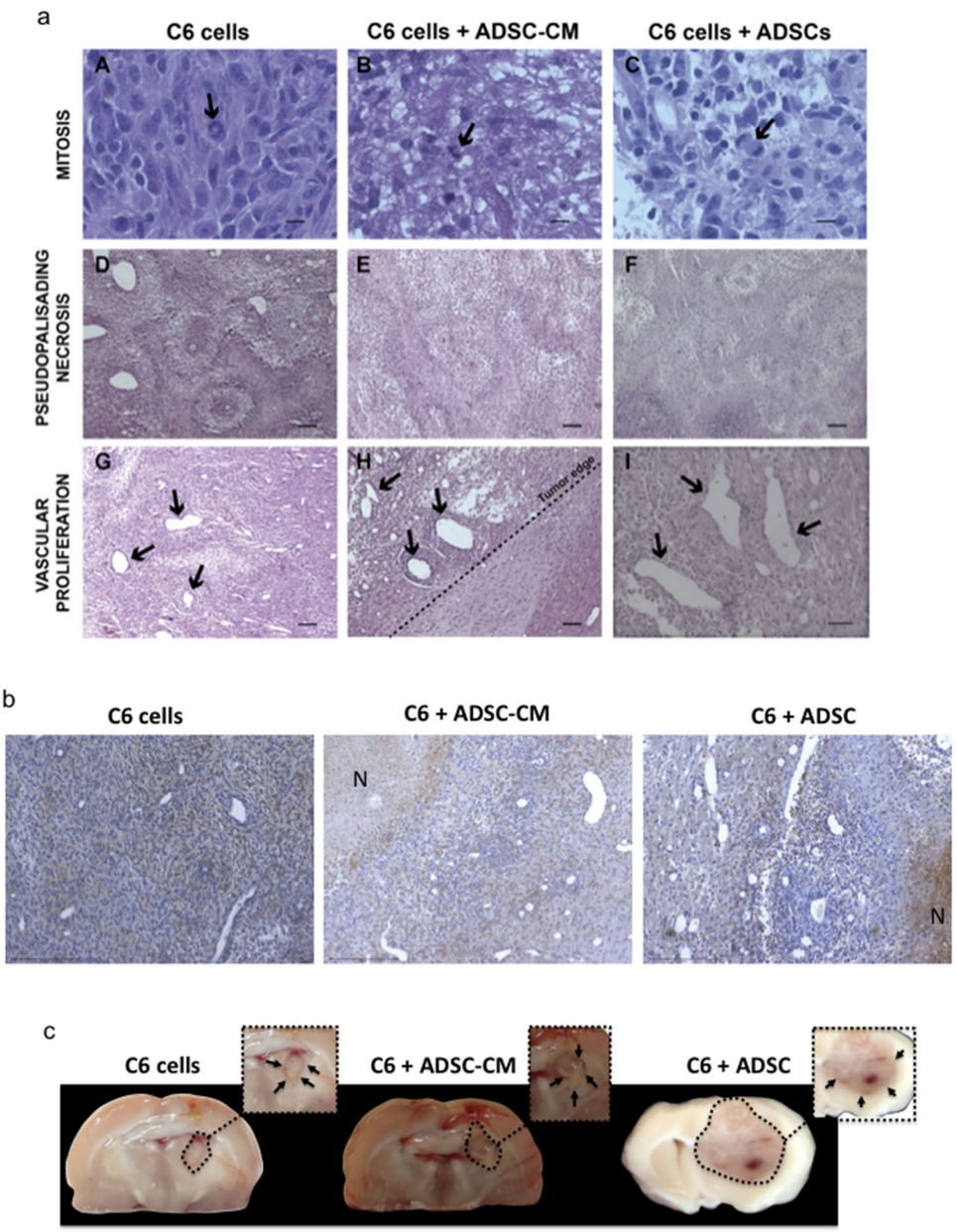

Fig. 2 Histological analysis of implanted gliomas. The sections of implanted rat glioma were stained with hematoxylin and eosin (H&E), as described in "Methods" Section. **a** Representative pictures of histological characteristics that define glioblastoma multiform, as seen in rats of Group 1 (C6) (**a**, **d**, **g**), Group 2 (C6 + ADSC-CM) (**b**, **e**, **h**) and Group 3 (C6 + ADSC) (**c**, **f**, **i**). Pseudopalisading necrosis, microvascular proliferation (arrows) and mitosis (arrows) were observed. Histological examination of tumors was performed in all animals. Scale bars = 10 µM (**a**, **b**, **c**,); 50 µM (**i**); 100 µM (**d**, **e**, **f**, **g**, **h**). **b** Representative pictures of CD73 immunohistochemical analysis. Scale bars = 200 µM. Necrosis areas were observed (N). **c** Representative photographs of rat brain slices of implanted gliomas of Group 1 (C6), Group 2 (C6 + ADSC-CM) and Group 3 (C6 + ADSC). The gliomas are marked with a circle

(C6+ADSC) developed larger tumors, when observed with naked eye (visual inspection), in relation to animals from other groups (Fig. 2c).

Cell Proliferation, Astrogliosis and EMT-Related Genes Expression in Glioma Tumors

Next, we tested whether ADSCs or ADSC-CM alters tumor cell volume through direct modulation of tumor cell proliferation. We found through Ki67 immunostaining that the proliferation rate of C6-derived gliomas did not statistically differ following treatment with ADSC-CM or co-injection with ADSCs (Fig. 3a–b). These data suggest that ADSC-CM treatment or co-injection with C6 and ADSCs, per se, does not, or is not sufficient to, modify the in vivo proliferation program of C6 tumor cells.

Brain tumors induce reactive astrogliosis and this process is associated with increased expression of GFAP. Therefore, we tested whether ADSCs or ADSC-CM could intensify GFAP expression in our model [32, 33]. In agreement with previous observations [34, 35], GFAP expression was highly upregulated at the tumor edge, forming a glial scar, whereas a reduced GFAP immunoreactivity was observed in the tumor bulk (Fig. 3c–d). However, in our experimental design, neither co-implantation of C6 cells+ADSCs nor exposure of C6 cells to the ADSC-CM demonstrated any difference in the density of GFAP immunopositive cells in tumor bulk, tumor edge

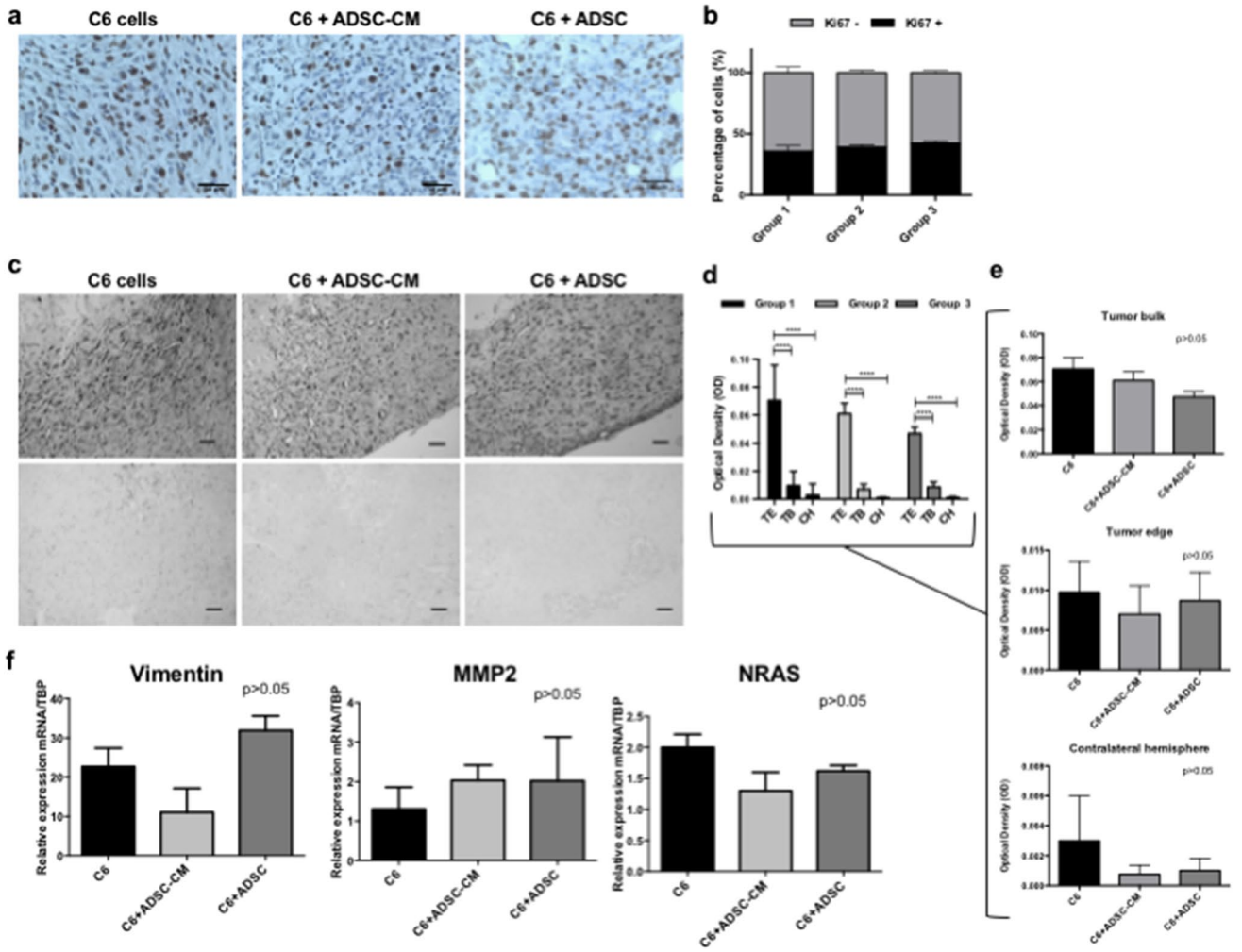

Fig. 3 Immunohistochemical staining and expression of EMT-related markers in implanted gliomas. **a** Representative pictures of immunohistochemical analysis. **b** Percentages of positive (Ki67 +) and negative (Ki67-) cells to brown nuclear expression of Ki67. **c** Representative pictures of immunohistochemical analysis of tumor bulk and edge of rats. **d**–**e** Optical Density Measurements, to evaluate GFAP immunoreactivity. **f** Quantitative PCR of vimentin, MMP2 and NRAS genes in tumors of rats. Quantitative PCR measurements of gene expression levels are normalized against TBP levels, and expressed relatively to the normal brain. *TB* tumor bulk, *TE* tumor edge, *CH* contralateral hemisphere. The results are presented as mean values ± SEM, as determined by one-way ANOVA followed by post-hoc comparisons (Tukey). *$p < 0.05$ indicates statistical difference from control. Scale bars = 10 μM (**a**); 100 μM (**c**)

and contralateral hemisphere, when compared with C6 cells-derived tumors (Fig. 3e).

EMT is a recognized process often involved in tumor progression, however, in this study, the expression of vimentin, MMP2 and NRAS were not different in tumors derived from C6 cells, C6+ADSC cells and C6 cells following treatment with ADSC-CM (Fig. 3f). Our data thus suggests that neither the physical presence nor molecules secreted by ADSCs are able to enhance the expression of these three EMT-related genes at RNA levels in vivo.

Co-Injection of C6 and ADSC Enhanced Tumor Volume In Vivo and Reduced the Animals Survival

After 20 days of cells implantation, the hematoxylin and eosin (H&E) analysis showed that 7 of 9 animals (78%) that received C6 cells presented a defined tumor mass, against 9 of 10 animals (90%) and 7 of 9 animals (88%) in the groups that received hMSC-CM-treated C6 tumor cells alone or untreated tumor cells mixed with ADSC, respectively. The other animals showed only cells with

characteristics of a residual tumor in the site of glioma implantation. Therefore, the analysis of the tumor volume was carried out exclusively in animals presenting a tumoral mass that could be quantified.

Animals of the C6+ADSC group presented larger tumors, when compared to the animals of the other groups (Fig. 2b and 4a). The mean of tumor volume in the C6+ADSC group was 146 mm^3 at 20 days after injection, in contrast to the C6-only group C6 pretreated with ADSC-CM groups, whose values were, respectively, 43 mm^3 and 63 mm^3 (Fig. 4a). To investigate whether the effect of ADSC on tumor volume was cell specific, we co-injected C6 cells with astrocytes, as these cells are naturally found in the brain tissue. The mean of tumor volume of this group was 117 mm^3. This analysis was performed only in three animals, but despite this, there were no statistical differences, when compared to group 1 (Fig. 4a).

In line with the tumor size data, long-term survival was shorter in animals that received C6+ADSCs in relation to the other groups, as animals of this group 3 died between days 20 and 22 after tumor implantation (Fig. 4b and Supplementary Table 3). In contrast, most animals of the other groups survived this experiment, not showing symptoms until the day of euthanasia.

In the animals that received co-injection of C6 cells and astrocytes, we confirmed that the presence of the astrocytes did not alter the characteristics of the tumors formed. The representative microscopic analysis revealed tumors with typical GBM characteristics (Fig. 4c, panel A). We also confirmed that the inoculation of astrocytes did not alter the presence of astrogliosis around the tumor (Fig. 4, panel B). At the same time, we observed that the astrocytes were efficiently inoculated into the rat brains, since, even in the animals that did not present defined tumor mass, we could observe the presence of astrocytes in the region of inoculation of the cells (Fig. 4c, panel C), when compared to other regions of the brain (Fig. 4, panel D).

Necrosis Analysis and Immunohistochemistry for CD45

In order to better understand the mechanism that led animals of the C6+ADSC group to develop larger tumors, a careful histopathological analysis was performed. We observed that the animals in the C6+ADSC group presented more areas of necrosis, when compared to the other groups (Fig. 5a–c). Furthermore, the same analysis evidenced that animals of the C6+ADSC group presented more infiltrate of immune cells into de tumor mass. This observation was confirmed by immunohistochemistry for CD45 (Fig. 5d–f and Supplementary Table 4).

Discussion

Although MSCs have been used as cellular delivery vehicles for antitumor agents in a broad variety of tumor types [5, 36–38], there is no consensus whether MSCs promote or inhibit tumor progression in vivo. However, it is becoming evident that stromal cells, including MSCs, play an indispensable role in the tumor microenvironment and cancer progression [8, 39, 40]. We, therefore, explored the in vivo effect of ADSCs and their conditioned medium in malignant glioma tumors to contribute with this understanding.

In our previous study in vitro, we showed that ADSC-CM promotes EMT-like process in C6 glioma cell line [21]. Nevertheless, here we showed that neither ADSC-CM nor ADSC were able to induce increased expression of EMT-related markers in vivo. Our results are consistent with the idea that the detection of EMT in vivo during disease progression is particularly difficult and remains a challenge of EMT program [41, 42]. This difficulty is mainly because EMT is a dynamic process, marked by the ability of cancer cells to remain in a hybrid stage, known as "incomplete" EMT, or even return their phenotype through mesenchymal to epithelial transition (MET). This dynamism is much more evident in a living organism with tumors enriched by stromal cells, than in a controlled environment of cell cultures [43]. Moreover, the process of EMT in GBM is quite unusual and some important characteristics of EMT are not observed in GBM [44].

Our pathological analysis demonstrated that the expression of Ki67 marker, an antigen expressed during G1, S, and G2/M phases in proliferating cells, was similar among the analyzed groups. This result indicates that the treatments were not able to change the C6 cell proliferation program. In accordance with our results, previous data of our group showed that, in vitro, hADSC-CM treatment also did not alter cell proliferation rate of human U87 GBM cell line [20]. In contrast, Zhu et al. reported that both human bone marrow-derived MSC (BMSCs) and their CM were able to promote human gastric tumor growth in a model of immunodeficient mouse [11]. However, it is important to consider differences in cell type and animal model used, mainly because in this case, cells were forced to adapt to a different microenvironment, with the absence of an immune system. Moreover, it is important to keep in mind that tissue-resident stem cells can also be recruited to the tumor microenvironment and to interact with tumor cells. For instance, ADSCs have been described to home to breast tumor site when co-injected locally and i.v in nude mice, interacting with tumor cells and promoting significantly faster cancer growth. The authors showed that ADSCs promote tumor cell motility,

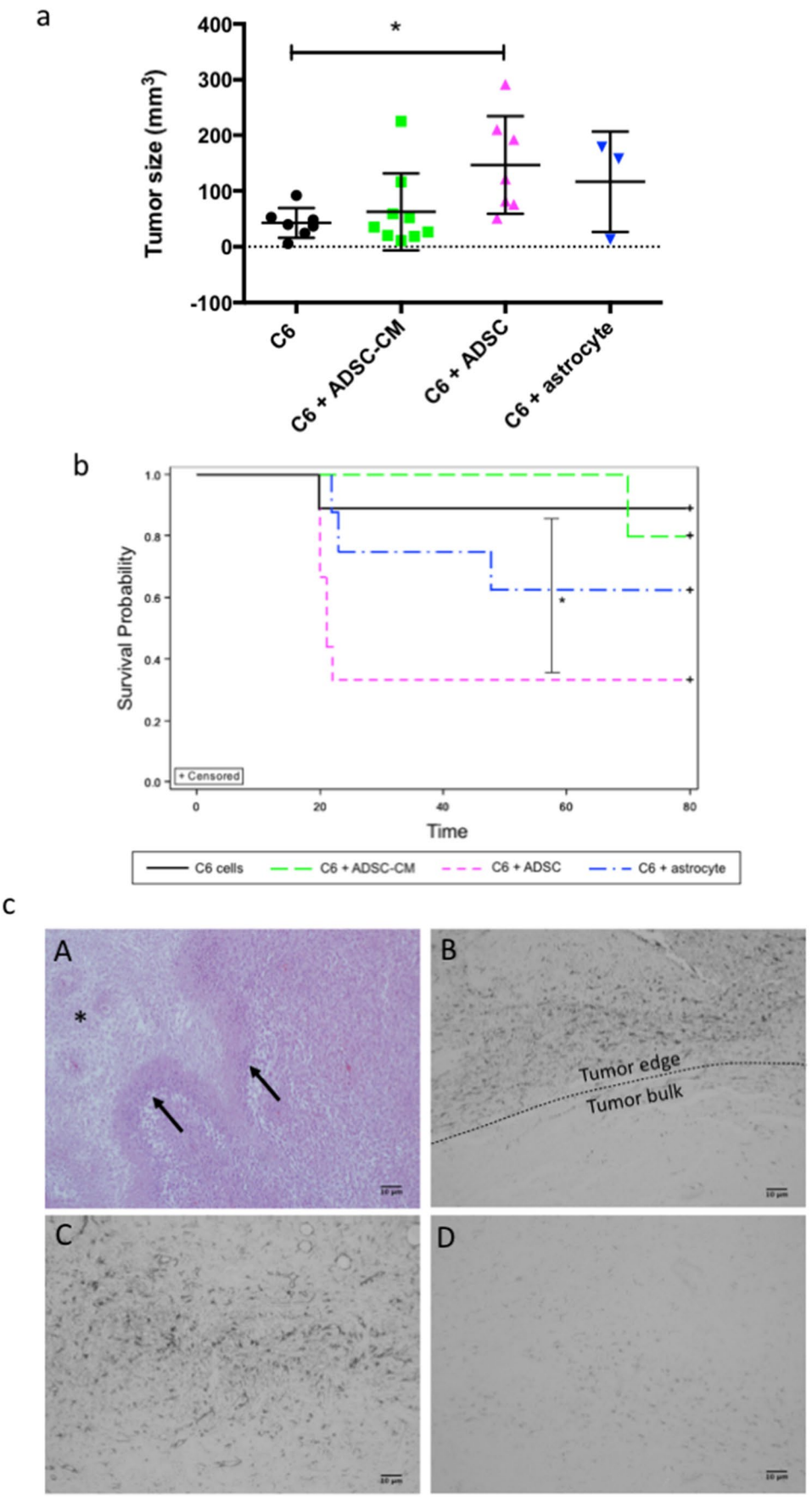

Fig. 4 Tumor volume of implanted gliomas and survival rate. Animals were treated, as described in "Methods" Section. The animals were killed 20 days after implantation of cells and glioma sections were dissected and analyzed for tumor size. **a** Tumor size quantification of implanted gliomas. **d** The animals were observed for 90 days after glioma implantation (n = minimum 5 animals per group). Survival curves were constructed by using the Kaplan–Meier method. **c** In the animals of Group 4, the tumors also exhibited pseudopalisading necrosis zone (asterisk), with presence of rapidly proliferating tumor cells (arrows). The tumor bulk was marked by a weak staining of GFAP (*A*) in comparison to tumor edge (*B*) and it is possible to observe a greater presence of astrocytes (GFAP +) (arrows) in the zone of injection of cells (*C*) in comparison to contralateral hemisphere of brain with normal presence of cells GFAP + (*D*)

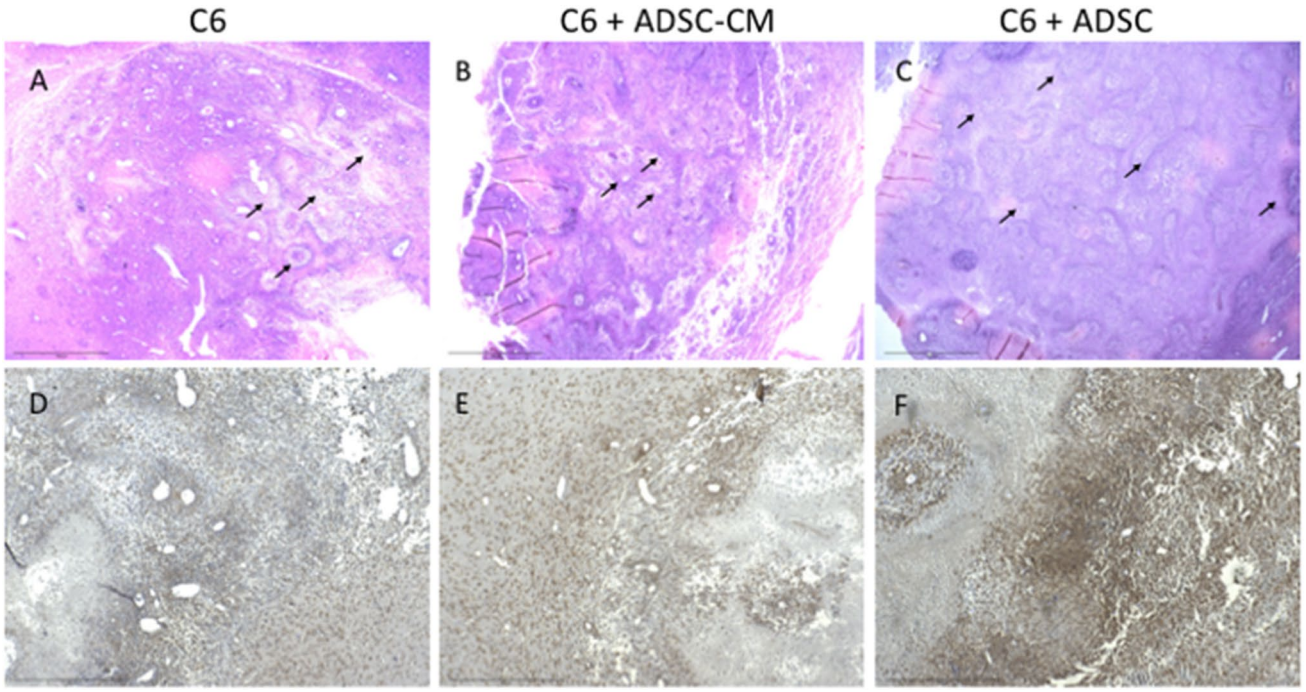

Fig. 5 Histopathological analysis of necrosis and immunohistochemistry for CD45. **a**–**c** Immunopathological analysis of necrosis areas. Scale bars = 1000 μM. **d**–**f** Representative pictures of immunohistochemical analysis for CD45. Scale bars = 500 μM

invasion and metastasis by secreting paracrine factors and by their ability to incorporate into tumor vessels and differentiate into endothelial cells [45]. In accordance with these findings, resident MSCs from lymphoma are also able to induce tumor growth by secretion of soluble factors and macrophage recruitment to tumor sites [46]. In lung cancer and gastric cancer were observed similar results, with endogenous stem cells being "educated" by tumor cells and acquiring tumor-promoting abilities [47, 48]. Recruited-MSCs are also capable of supporting tumor growth and aggressiveness through the increase of proliferation and self-renewal of glioma stem cells via IL-6 release [49].

Diffuse gliomas induce brain injury and stimulate their own process of gliosis or reactive astrocytosis creating an altered brain microenvironment, more permissive to tumor growth/invasion [33, 50]. Here, reactive astrogliosis was observed at the periphery of tumors, forming a gliotic margin. Nonetheless, the level of GFAP expression on the tumor edge was similar in all experimental groups. In accordance with these results, our observations demonstrate that the treatment of C6 cells with CM and co-injection with ADSCs did not alter histological characteristics of the tumors.

Surprisingly, although proliferation rate and astrogliosis reaction were not altered in our model, animals co-injected with C6 cells and ADSCs developed larger tumors, when compared with animals that received untreated C6 tumor cells alone or CM-treated C6 tumor cells alone. These results suggest that other events than the proliferative rate accounts for the difference in tumor volume. Several researchers have suggested the capacity of tumors to release factors and "educate" their stromal cells and induce malignant transformation of MSCs, both in vitro and in vivo [51–53]. Liu et al. [51] showed that rat MSCs underwent malignant transformation after indirect co-culture with C6 cells in vitro and formed large tumors when transplanted subcutaneously into immuno-deficient mice [51]. Bexell and colleagues injected rat BMSCs intratumorally in established orthotopic rat GBM tumors, and observed that these cells migrate to tumor endothelium, acting like pericytes within tumors [4], possibly supporting vessel function and tumor growth and even indirectly, the infiltrative capacity of tumors [54]. Glioma stem cells (GSCs) are also able to induce malignant transformation of BMSCs by activating TERT expression. Besides, transformed BMSCs are able to generate subcutaneous tumors when transplanted in athymic nude mice [55]. In addition, C6 glioma-conditioned medium (GCM) induces malignant transformation of MSCs. The transformed MSCs exhibited tumor cell characteristics in vitro and were highly tumorigenic when injected in mice, even in the absence of tumor cells [56]. Since cancer cells are known to be highly fusogenic, another mechanism that could be an explanation to our results, is the cell fusion that has been recently suggested, as an explanation for stem cell plasticity in tumor microenvironment [49–52]. It has already been shown that the spontaneous fusion, between embryonic stem cells and

central nervous system (CNS) cells, generates hybrid pluripotent cells [53], suggesting the acquisition of a special plasticity that could allow them to differentiate in tumor cells.

The MSCs that compose the tumor microenvironment in certain circumstances become reactive stroma cells and finally, tumor-associated stromal cells, expressing higher levels of extracellular matrix proteins. These cells also release pro-tumorigenic factors, including IL-6, among others, which recruit other pro-tumorigenic cells. In particular, IL-6, is a pro-inflammatory cytokine able to modify stromal cell function, migration and EMT. Inside this pro-tumorigenic microenvironment, stromal cells are still able to transdifferentiate, such as fibroblasts which transdifferentiate into activated myofibroblast during formation of the reactive stroma [57]. MSCs have a high capacity to differentiate into endothelial cells, macrophages and cancer-associated fibroblasts, contributing to proliferation of tumor stroma [58]. Interestingly, these stromal cells can be "corrupted" by the tumor microenvironment. Fomchenko et al. showed the stromal corruption using an animal model of GBM in which they recognized non-tumor stromal cells with genetic mutations similar to the glioma cell. This means that stromal cells present in tumor microenvironment can be corrupted to become genuine tumor [10].

We observed that the group of animals that received C6+ADSC developed tumors with larger necrosis areas, which is considered a poor prognostic factor. Our hypothesis is that MSC might be part and induce a peritumoral stroma strongly permissive to fast tumor growth and consequently formation of necrotic areas. Vakkila et al. have suggested that adult cancers result from rounds of disordered and spontaneous necrotic cell death followed by epithelial proliferation and immune suppression. The necrotic cell death stimulates inflammatory mechanisms related to angiogenesis, stromagenesis and epithelial proliferation, thus inducing tumor growth [59]. In GBM, pseudopalisading cells overexpress hypoxia-inducible factor (HIF-1) and secrete proangiogenic factors, providing microvascular hyperplasia, new vasculature and promoting peripheral tumor expansion [60]. Furthermore, necrosis is associated with immune response, impacting directly on tumor growth. Necrotic cells secrete a factor known as High-mobility group box 1 protein (HMGB1), promoting recruitment of inflammatory cells. In GBM animal models, the blockade of HMGB1 receptor inhibits tumor growth [59, 61].

Not only necrotic cells have an important immunomodulatory role, but stem cells themselves have immunosuppressive or immunomodulatory properties, possibly suppressing cells of the adaptive immune system and thereby promoting tumor growth. Many cytokines released by MSCs, such as TGFβ, IL10, nitric oxide, prostaglandin E2, and indoleamine 2,3-dioxygenase, are related to immunomodulation [58]. MSC are able to support breast cancer cells by increasing regulatory T-cell activity [62]. Similarly, immunomodulatory effects were observed in prostate cancer, where the inflammatory cytokine IL1α induces the immunosuppressive function of MSCs, enabling cancer cells to escape from immunosurveillance [63]. Interestingly, the presence of MSCs in cervical cancer inhibits the recognition of cancer cells by cytotoxic T lymphocytes, providing immune protection to tumor cells [64].

MSCs are also responsible for the recruitment and interaction with cells from innate immunity, especially macrophages, neutrophils and myeloid-derived suppressor cells (MDSCs), to promote an anti-inflammatory state and thereby enhance tumor growth and metastasis. It has been observed that MSCs from bone marrow and human placenta induce monocytes to convert M1 inflammatory macrophages to anti-inflammatory M2 macrophages [65]. In addition, MSC can induce macrophages to secrete TGFβ, a molecule with anti-inflammatory effect, inducing Treg cells and CD8+T cells with a suppressive phenotype [66].

Taking into account the important role of necrosis and the presence of MSCs in the tumor mass and to better understand whether ADSCs could affect the immune population of cells into the tumor, we performed CD45 immunohistochemistry in tumor slides. CD45 is also called leukocyte common antigen (LCA) and is broadly used to confirm the presence of inflammatory cells into the tumor. Interestingly, C6+ADSC group presented a much higher DC45 staining when compared to the other groups. As CD45 is expressed in myeloid-derived suppressor cells (MDSCs) and regulatory T cells (T Regs) [67], we can hypothesize that the immune cells that are recruited to the glioma microenvironment, both by factors released by necrotic cells or by tumor stem cells themselves, must have an immunosuppressive character, which favors tumor progression, mainly considering the well-known and studied immunosuppressive properties of ADSC.

As the lethality of brain tumors seems in part from the pressure onto essential brain regions, the increase in tumor volume induced by the combination of necrosis and immune infiltration, even without an increase in cancer cell proliferation can be responsible for the shorter survival of the C6+ADSC group compared to the other groups.

We also questioned whether this effect observed in tumor volume would be specifically related to ADSCs or whether any cell type could produce the same increase in tumor volume. Therefore, we co-injected C6 + primary rat astrocytes into rat brains and observed that astrocytes were not able to cause the same effect in tumor volume, when compared to ADSCs. When the brains were analyzed after euthanasia, it was possible observe the presence of astrocytes in cell inoculation zone, as evidenced by GFAP staining, however, without significant consequence in tumor development. This result proves that the effect of ADSC in tumor volume is

cell-specific. ADSCs seem to induce their modulatory roles without a large increase in cell number, as suggested by the low staining with CD73, a well-known marker of MSCs in general. This result also indicates that the increased volume is not due to the proliferation of the ADSCs but due to their effects on the behavior of the tumor cells and the components of the tumor microenvironment.

Finally, our main objective was to know whether the increase in the tumor volume initiated by the ADSCs was permanent or temporary, and whether it could impact on animal survival. Our results showed that the animals that received C6 in combination with ADSCs presented an evident lower survival, when compared to other groups analyzed. The observation that ADSCs can enhance the tumor volume in vivo is an important finding that provides clear evidence for the need of caution when using ADSCs for tumor therapies. Therefore, the understanding of the fate and functions of MSCs in tumor sites in vivo, as well as their intricate crosstalk with cancer cells, is essential to ensure the safe use of MSCs to treat different types of cancers. A fuller understanding of the mechanisms by which MSCs interact with cancer cells will bring immense benefits to the field of oncology. The wide knowledge about the role of MSCs in cancer development will allow not only the improvement of MSC-based therapies, but also, it will open up opportunities for developing effective therapies for preventing tumor progression.

Supplementary Information The online version contains supplementary material available at https://doi.org/10.1007/s12015-021-10227-6.

Acknowledgements The authors would like to thank Giuliano Rizzotto Guimarães, Terezinha Stein and Rosalva Thereza Meurer (Laboratório de Pesquisa em Patologia, UFCSPA) for excellent technical assistance with histological analysis and M.Sc. Cristiano Rodrigues for his assistance in animal facility. The authors also gratefully acknowledge veterinarians Drs. Fernanda Bastos de Mello and Joana Fisch for animal assistance.

Author Contribution ICI performed cell culture, in vivo experiments, and wrote the manuscript. LRB and JHA assisted with in vivo glioma model. APSB performed RT-qPCR assays. EB contributed with the glioma model and with the interpretation of the results; FLR assisted with animal perfusions; MCF assisted with histological analysis and the interpretation of data; RCSA analyzed the pathology of gliomas; LLX contributed with GFAP immunohistochemistry quantification; PAB assisted with the statistics and interpretation of the results; MRW got and coordinate the grants, supervised the experiments, assisted in drafting and critical reading. GL supervised the experiments and assisted with critical reading. All the authors discussed the results and contributed to the writing of the manuscript.

Funding APSB is recipient of PNPD fellowship from CAPES (Coordenação de Aperfeiçoamento de Pessoal de Nível Superior); MRW, GL, EB and LLX are recipients of research fellowship from CNPq (Conselho Nacional de Desenvolvimento Científico e Tecnológico); ICI was recipient of PDJ and LRB was recipient of DTI-B fellowship from CNPq. This study was supported by CNPq, MS-SCTIE-Decit/CNPq nº 12/2018 (441575/2018-8) and MS-SCTIE-DECIT-DGITIS-CGCIS/CNPq nº 26/2020 (442586/2020–5); and by Fundação de Amparo à Pesquisa do Estado do Rio Grande do Sul—Brasil (FAPERGS/CAPES 06/2018—Programa de Internacionalização da pós-graduação no RS (19/2551-0000679-9).

Declarations

Conflict of interest The authors have no conflict of interest to declare.

Ethics Approval The protocols used in this study were approved by the Ethics Committee on Animal Use (CEUA) of Universidade Federal de Ciências da Saúde de Porto Alegre (UFCSPA), under the number **104/11**, following the resolutions of the CONCEA (Conselho Nacional de Controle de Experimentação Animal). The NIH ''Guide for the Care and Use of Laboratory Animals'' (NIH publication nº 80–23, revised 1996) was followed in all experiments. The surgeries were performed with all efforts to minimize the animals suffering.

Informed Consent The authors are alone responsible for the content and writing of the paper. All authors reviewed and approved the final version of the manuscript.

References

1. Jones, T. S., & Holland, E. C. (2012). Standard of care therapy for malignant glioma and its effect on tumor and stromal cells. *Oncogene, 31*(16), 1995–2006. https://doi.org/10.1038/onc.2011.398
2. Lima, F. R. S., Kahn, S. A., Soletti, R. C., Biasoli, D., Alves, T., da Fonseca, A. C. C., … Moura-Neto, V. (2012). Glioblastoma: Therapeutic challenges, what lies ahead. *Biochimica Et Biophysica Acta, 1826*(2), 338–349. https://doi.org/10.1016/j.bbcan.2012.05.004
3. Mitchell, J. B., McIntosh, K., Zvonic, S., Garrett, S., Floyd, Z. E., Kloster, A., … Gimble, J. M. (2006). Immunophenotype of human adipose-derived cells: Temporal changes in stromal-associated and stem cell-associated markers. *Stem Cells (Dayton, Ohio), 24*(2), 376–385. https://doi.org/10.1634/stemcells.2005-0234
4. Bexell, D., Svensson, A., & Bengzon, J. (2013). Stem cell-based therapy for malignant glioma. *Cancer Treatment Reviews, 39*(4), 358–365. https://doi.org/10.1016/j.ctrv.2012.06.006
5. Cavarretta, I. T., Altanerova, V., Matuskova, M., Kucerova, L., Culig, Z., & Altaner, C. (2010). Adipose tissue-derived mesenchymal stem cells expressing prodrug-converting enzyme inhibit human prostate tumor growth. *Molecular Therapy: The Journal of the American Society of Gene Therapy, 18*(1), 223–231. https://doi.org/10.1038/mt.2009.237
6. Kucerova, L., Altanerova, V., Matuskova, M., Tyciakova, S., & Altaner, C. (2007). Adipose tissue-derived human mesenchymal stem cells mediated prodrug cancer gene therapy. *Cancer Research, 67*(13), 6304–6313. https://doi.org/10.1158/0008-5472.CAN-06-4024
7. Altanerova, V., Cihova, M., Babic, M., Rychly, B., Ondicova, K., Mravec, B., & Altaner, C. (2012). Human adipose tissue-derived mesenchymal stem cells expressing yeast cytosinedeaminase: Uracil phosphoribosyltransferase inhibit intracerebral rat glioblastoma. *International Journal of Cancer, 130*(10), 2455–2463. https://doi.org/10.1002/ijc.26278
8. Barcellos-de-Souza, P., Gori, V., Bambi, F., & Chiarugi, P. (2013). Tumor microenvironment: Bone marrow-mesenchymal stem cells

as key players. *Biochimica Et Biophysica Acta, 1836*(2), 321–335. https://doi.org/10.1016/j.bbcan.2013.10.004
9. Adjei, I. M., & Blanka, S. (2015). Modulation of the tumor microenvironment for cancer treatment: A biomaterials approach. *Journal of Functional Biomaterials, 6*(1), 81–103. https://doi.org/10.3390/jfb6010081
10. Fomchenko, E. I., Dougherty, J. D., Helmy, K. Y., Katz, A. M., Pietras, A., Brennan, C., … Holland, E. C. (2011). Recruited cells can become transformed and overtake PDGF-induced murine gliomas in vivo during tumor progression. *PloS ONE, 6*(7), e20605. https://doi.org/10.1371/journal.pone.0020605
11. Zhu, W., Huang, L., Li, Y., Qian, H., Shan, X., Yan, Y., … Xu, W.-R. (2011). Mesenchymal stem cell-secreted soluble signaling molecules potentiate tumor growth. *Cell Cycle (Georgetown, Tex.), 10*(18), 3198–3207. https://doi.org/10.4161/cc.10.18.17638
12. Chien, L.-Y., Hsiao, J.-K., Hsu, S.-C., Yao, M., Lu, C.-W., Liu, H.-M., … Huang, D.-M. (2011). In vivo magnetic resonance imaging of cell tropism, trafficking mechanism, and therapeutic impact of human mesenchymal stem cells in a murine glioma model. *Biomaterials, 32*(12), 3275–3284. https://doi.org/10.1016/j.biomaterials.2011.01.042
13. Giuffrida, D., Rogers, I. M., Nagy, A., Calogero, A. E., Brown, T. J., & Casper, R. F. (2009). Human embryonic stem cells secrete soluble factors that inhibit cancer cell growth. *Cell Proliferation, 42*(6), 788–798. https://doi.org/10.1111/j.1365-2184.2009.00640.x
14. Sun, B., Roh, K.-H., Park, J.-R., Lee, S.-R., Park, S.-B., Jung, J.-W., … Kang, K.-S. (2009). Therapeutic potential of mesenchymal stromal cells in a mouse breast cancer metastasis model. *Cytotherapy, 11*(3), 289–298. https://doi.org/10.1080/14653240902807026
15. Karnoub, A. E., Dash, A. B., Vo, A. P., Sullivan, A., Brooks, M. W., Bell, G. W., … Weinberg, R. A. (2007). Mesenchymal stem cells within tumour stroma promote breast cancer metastasis. *Nature, 449*(7162), 557–563. https://doi.org/10.1038/nature06188
16. De Luca, A., Lamura, L., Gallo, M., Maffia, V., & Normanno, N. (2012). Mesenchymal stem cell-derived interleukin-6 and vascular endothelial growth factor promote breast cancer cell migration. *Journal of Cellular Biochemistry, 113*(11), 3363–3370. https://doi.org/10.1002/jcb.24212
17. Beckermann, B. M., Kallifatidis, G., Groth, A., Frommhold, D., Apel, A., Mattern, J., … Herr, I. (2008). VEGF expression by mesenchymal stem cells contributes to angiogenesis in pancreatic carcinoma. *British Journal of Cancer, 99*(4), 622–631. https://doi.org/10.1038/sj.bjc.6604508
18. Kidd, S., Spaeth, E., Klopp, A., Andreeff, M., Hall, B., & Marini, F. C. (2008). The (in) auspicious role of mesenchymal stromal cells in cancer: Be it friend or foe. *Cytotherapy, 10*(7), 657–667. https://doi.org/10.1080/14653240802486517
19. Wong, R. S. Y. (2011). Mesenchymal stem cells: Angels or demons? *Journal of Biomedicine & Biotechnology, 2011*, 459510. https://doi.org/10.1155/2011/459510
20. Onzi, G. R., Ledur, P. F., Hainzenreder, L. D., Bertoni, A. P. S., Silva, A. O., Lenz, G., & Wink, M. R. (2016). Analysis of the safety of mesenchymal stromal cells secretome for glioblastoma treatment. *Cytotherapy, 18*(7), 828–837. https://doi.org/10.1016/j.jcyt.2016.03.299
21. Iser, I. C., Ceschini, S. M., Onzi, G. R., Bertoni, A. P. S., Lenz, G., & Wink, M. R. (2016). Conditioned medium from adipose-derived stem cells (ADSCs) promotes epithelial-to-mesenchymal-like transition (EMT-Like) in glioma cells in vitro. *Molecular Neurobiology, 53*(10), 7184–7199. https://doi.org/10.1007/s12035-015-9585-4
22. Wink, M. R., Braganhol, E., Tamajusuku, A. S. K., Casali, E. A., Karl, J., Barreto-Chaves, M. L., … Battastini, A. M. O. (2003). Extracellular adenine nucleotides metabolism in astrocyte cultures from different brain regions. *Neurochemistry International, 43*(7), 621–628. https://doi.org/10.1016/s0197-0186(03)00094-9
23. da Silva Meirelles, L., Chagastelles, P. C., & Nardi, N. B. (2006). Mesenchymal stem cells reside in virtually all post-natal organs and tissues. *Journal of Cell Science, 119*(Pt 11), 2204–2213. https://doi.org/10.1242/jcs.02932
24. Takano, T., Lin, J. H., Arcuino, G., Gao, Q., Yang, J., & Nedergaard, M. (2001). Glutamate release promotes growth of malignant gliomas. *Nature Medicine, 7*(9), 1010–1015. https://doi.org/10.1038/nm0901-1010
25. Morrone, F. B., Oliveira, D. L., Gamermann, P., Stella, J., Wofchuk, S., Wink, M. R., … Battastini, A. M. O. (2006). In vivo glioblastoma growth is reduced by apyrase activity in a rat glioma model. *BMC Cancer, 6*, 226. https://doi.org/10.1186/1471-2407-6-226
26. Xavier, L. L., Viola, G. G., Ferraz, A. C., Da Cunha, C., Deonizio, J. M. D., Netto, C. A., & Achaval, M. (2005). A simple and fast densitometric method for the analysis of tyrosine hydroxylase immunoreactivity in the substantia nigra pars compacta and in the ventral tegmental area. *Brain Research. Brain Research Protocols, 16*(1–3), 58–64. https://doi.org/10.1016/j.brainresprot.2005.10.002
27. Azambuja, J. H., Schuh, R. S., Michels, L. R., Gelsleichter, N. E., Beckenkamp, L. R., Iser, I. C., … Braganhol, E. (2020). Nasal administration of cationic nanoemulsions as CD73-siRNA delivery system for glioblastoma treatment: A new therapeutical approach. *Molecular Neurobiology, 57*(2), 635–649. https://doi.org/10.1007/s12035-019-01730-6
28. Azambuja, J. H., Gelsleichter, N. E., Beckenkamp, L. R., Iser, I. C., Fernandes, M. C., Figueiró, F., … Braganhol, E. (2019). CD73 downregulation decreases in vitro and in vivo glioblastoma growth. *Molecular Neurobiology, 56*(5), 3260–3279. https://doi.org/10.1007/s12035-018-1240-4
29. Braganhol, E., Zanin, R. F., Bernardi, A., Bergamin, L. S., Cappellari, A. R., Campesato, L. F., … Battastini, A. M. O. (2012). Overexpression of NTPDase2 in gliomas promotes systemic inflammation and pulmonary injury. *Purinergic Signalling, 8*(2), 235–243. https://doi.org/10.1007/s11302-011-9276-1
30. Doblas, S., He, T., Saunders, D., Pearson, J., Hoyle, J., Smith, N., … Towner, R. A. (2010). Glioma morphology and tumor-induced vascular alterations revealed in seven rodent glioma models by in vivo magnetic resonance imaging and angiography. *Journal of magnetic resonance imaging: JMRI, 32*(2), 267–275. https://doi.org/10.1002/jmri.22263
31. Gieryng, A., Pszczolkowska, D., Walentynowicz, K. A., Rajan, W. D., & Kaminska, B. (2017). Immune microenvironment of gliomas. *Laboratory Investigation; A Journal of Technical Methods and Pathology*, *97*(5), 498–518. https://doi.org/10.1038/labinvest.2017.19
32. Pisati, F., Belicchi, M., Acerbi, F., Marchesi, C., Giussani, C., Gavina, M., … Torrente, Y. (2007). Effect of human skin-derived stem cells on vessel architecture, tumor growth, and tumor invasion in brain tumor animal models. *Cancer Research, 67*(7), 3054–3063. https://doi.org/10.1158/0008-5472.CAN-06-1384
33. Chekhonin, V. P., Baklaushev, V. P., Yusubalieva, G. M., Pavlov, K. A., Ukhova, O. V., & Gurina, O. I. (2007). Modeling and immunohistochemical analysis of C6 glioma in vivo. *Bulletin of Experimental Biology and Medicine, 143*(4), 501–509. https://doi.org/10.1007/s10517-007-0167-y
34. Wilhelmsson, U., Eliasson, C., Bjerkvig, R., & Pekny, M. (2003). Loss of GFAP expression in high-grade astrocytomas does not contribute to tumor development or progression. *Oncogene, 22*(22), 3407–3411. https://doi.org/10.1038/sj.onc.1206372
35. Le, D. M., Besson, A., Fogg, D. K., Choi, K.-S., Waisman, D. M., Goodyer, C. G., … Yong, V. W. (2003). Exploitation of astrocytes by glioma cells to facilitate invasiveness: A mechanism involving

matrix metalloproteinase-2 and the urokinase-type plasminogen activator-plasmin cascade. *The Journal of Neuroscience: The Official Journal of the Society for Neuroscience, 23*(10), 4034–4043.
36. Bak, X. Y., Lam, D. H., Yang, J., Ye, K., Wei, E. L. X., Lim, S. K., & Wang, S. (2011). Human embryonic stem cell-derived mesenchymal stem cells as cellular delivery vehicles for prodrug gene therapy of glioblastoma. *Human Gene Therapy, 22*(11), 1365–1377. https://doi.org/10.1089/hum.2010.212
37. Kucerova, L., Matuskova, M., Pastorakova, A., Tyciakova, S., Jakubikova, J., Bohovic, R., … Altaner, C. (2008). Cytosine deaminase expressing human mesenchymal stem cells mediated tumour regression in melanoma bearing mice. *The Journal of Gene Medicine, 10*(10), 1071–1082. https://doi.org/10.1002/jgm.1239
38. Stoff-Khalili, M. A., Rivera, A. A., Mathis, J. M., Banerjee, N. S., Moon, A. S., Hess, A., … Curiel, D. T. (2007). Mesenchymal stem cells as a vehicle for targeted delivery of CRAds to lung metastases of breast carcinoma. *Breast Cancer Research and Treatment, 105*(2), 157–167. https://doi.org/10.1007/s10549-006-9449-8
39. Guan, J., & Chen, J. (2013). Mesenchymal stem cells in the tumor microenvironment. *Biomedical Reports, 1*(4), 517–521. https://doi.org/10.3892/br.2013.103
40. Zhang, Y., Daquinag, A., Traktuev, D. O., Amaya-Manzanares, F., Simmons, P. J., March, K. L., … Kolonin, M. G. (2009). White adipose tissue cells are recruited by experimental tumors and promote cancer progression in mouse models. *Cancer Research, 69*(12), 5259–5266. https://doi.org/10.1158/0008-5472.CAN-08-3444
41. Lee, J. M., Dedhar, S., Kalluri, R., & Thompson, E. W. (2006). The epithelial-mesenchymal transition: New insights in signaling, development, and disease. *The Journal of Cell Biology, 172*(7), 973–981. https://doi.org/10.1083/jcb.200601018
42. Thiery, J. P., & Chopin, D. (1999). Epithelial cell plasticity in development and tumor progression. *Cancer Metastasis Reviews, 18*(1), 31–42. https://doi.org/10.1023/a:1006256219004
43. Strauss, R., Hamerlik, P., Lieber, A., & Bartek, J. (2012). Regulation of stem cell plasticity: Mechanisms and relevance to tissue biology and cancer. *Molecular Therapy: The Journal of the American Society of Gene Therapy, 20*(5), 887–897. https://doi.org/10.1038/mt.2012.2
44. Iser, I. C., Pereira, M. B., Lenz, G., & Wink, M. R. (2017). The epithelial-to-mesenchymal transition-like process in glioblastoma: An updated systematic review and in silico investigation. *Medicinal Research Reviews, 37*(2), 271–313. https://doi.org/10.1002/med.21408
45. Muehlberg, F. L., Song, Y.-H., Krohn, A., Pinilla, S. P., Droll, L. H., Leng, X., … Alt, E. U. (2009). Tissue-resident stem cells promote breast cancer growth and metastasis. *Carcinogenesis, 30*(4), 589–597. https://doi.org/10.1093/carcin/bgp03
46. Ren, G., Liu, Y., Zhao, X., Zhang, J., Zheng, B., Yuan, Z.-R., … Shi, Y. (2014). Tumor resident mesenchymal stromal cells endow naïve stromal cells with tumor-promoting properties. *Oncogene, 33*(30), 4016–4020. https://doi.org/10.1038/onc.2013.387
47. Sai, B., Dai, Y., Fan, S., Wang, F., Wang, L., Li, Z., … Xiang, J. (2019). Cancer-educated mesenchymal stem cells promote the survival of cancer cells at primary and distant metastatic sites via the expansion of bone marrow-derived-PMN-MDSCs. *Cell Death & Disease, 10*(12), 941. https://doi.org/10.1038/s41419-019-2149-1
48. Kim, E.-K., Kim, H.-J., Yang, Y.-I., Kim, J. T., Choi, M.-Y., Choi, C. S., … Cheong, S.-H. (2013). Endogenous gastric-resident mesenchymal stem cells contribute to formation of cancer stroma and progression of gastric cancer. *Korean Journal of Pathology, 47*(6), 507–518. https://doi.org/10.4132/KoreanJPathol.2013.47.6.507
49. Hossain, A., Gumin, J., Gao, F., Figueroa, J., Shinojima, N., Takezaki, T., … Lang, F. F. (2015). Mesenchymal stem cells isolated from human gliomas increase proliferation and maintain stemness of glioma stem cells through the IL-6/gp130/STAT3 pathway. *Stem Cells (Dayton, Ohio), 33*(8), 2400–2415. https://doi.org/10.1002/stem.2053
50. Fitzgerald, D. P., Palmieri, D., Hua, E., Hargrave, E., Herring, J. M., Qian, Y., … Steeg, P. S. (2008). Reactive glia are recruited by highly proliferative brain metastases of breast cancer and promote tumor cell colonization. *Clinical & Experimental Metastasis, 25*(7), 799–810. https://doi.org/10.1007/s10585-008-9193-z
51. Liu, J., Zhang, Y., Bai, L., Cui, X., & Zhu, J. (2012). Rat bone marrow mesenchymal stem cells undergo malignant transformation via indirect co-cultured with tumour cells. *Cell Biochemistry and Function, 30*(8), 650–656. https://doi.org/10.1002/cbf.2844
52. Røsland, G. V., Svendsen, A., Torsvik, A., Sobala, E., McCormack, E., Immervoll, H., … Schichor, C. (2009). Long-term cultures of bone marrow-derived human mesenchymal stem cells frequently undergo spontaneous malignant transformation. *Cancer Research, 69*(13), 5331–5339. https://doi.org/10.1158/0008-5472.CAN-08-4630
53. Pan, Q., Fouraschen, S. M. G., de Ruiter, P. E., Dinjens, W. N. M., Kwekkeboom, J., Tilanus, H. W., & van der Laan, L. J. W. (2014). Detection of spontaneous tumorigenic transformation during culture expansion of human mesenchymal stromal cells. *Experimental Biology and Medicine (Maywood, N.J.), 239*(1), 105–115. https://doi.org/10.1177/1535370213506802
54. Cheng, L., Huang, Z., Zhou, W., Wu, Q., Donnola, S., Liu, J. K., … Bao, S. (2013). Glioblastoma stem cells generate vascular pericytes to support vessel function and tumor growth. *Cell, 153*(1), 139–152. https://doi.org/10.1016/j.cell.2013.02.021
55. Zhao, Y., Chen, J., Dai, X., Cai, H., Ji, X., Sheng, Y., … Dong, J. (2017). Human glioma stem-like cells induce malignant transformation of bone marrow mesenchymal stem cells by activating TERT expression. *Oncotarget*, *8*(61), 104418–104429. https://doi.org/10.18632/oncotarget.22301
56. Tan, B., Shen, L., Yang, K., Huang, D., Li, X., Li, Y., … Zhu, J. (2018). C6 glioma-conditioned medium induces malignant transformation of mesenchymal stem cells: Possible role of S100B/RAGE pathway. *Biochemical and Biophysical Research Communications, 495*(1), 78–85. https://doi.org/10.1016/j.bbrc.2017.10.071
57. Bussard, K. M., Mutkus, L., Stumpf, K., Gomez-Manzano, C., & Marini, F. C. (2016). Tumor-associated stromal cells as key contributors to the tumor microenvironment. *Breast Cancer Research: BCR, 18*(1), 84. https://doi.org/10.1186/s13058-016-0740-2
58. Ahn, S. Y. (2020). The role of MSCs in the tumor microenvironment and tumor progression. *Anticancer Research*, *40*(6), 3039–3047. https://doi.org/10.21873/anticanres.14284
59. Vakkila, J., & Lotze, M. T. (2004). Inflammation and necrosis promote tumour growth. *Nature Reviews. Immunology, 4*(8), 641–648. https://doi.org/10.1038/nri1415
60. Rong, Y., Durden, D. L., Van Meir, E. G., & Brat, D. J. (2006). "Pseudopalisading" necrosis in glioblastoma: A familiar morphologic feature that links vascular pathology, hypoxia, and angiogenesis. *Journal of Neuropathology and Experimental Neurology, 65*(6), 529–539. https://doi.org/10.1097/00005072-200606000-00001
61. Yee, P. P., Wei, Y., Kim, S.-Y., Lu, T., Chih, S. Y., Lawson, C., … Li, W. (2020). Neutrophil-induced ferroptosis promotes tumor necrosis in glioblastoma progression. *Nature Communications*, 11(1), 5424. https://doi.org/10.1038/s41467-020-19193-y
62. Patel, S. A., Meyer, J. R., Greco, S. J., Corcoran, K. E., Bryan, M., & Rameshwar, P. (2010). Mesenchymal stem cells protect breast cancer cells through regulatory T cells: Role of mesenchymal stem cell-derived TGF-beta. *Journal of Immunology (Baltimore, Md.: 1950), 184*(10), 5885–5894. https://doi.org/10.4049/jimmunol.0903143

63. Cheng, J., Li, L., Liu, Y., Wang, Z., Zhu, X., & Bai, X. (2012). Interleukin-1α induces immunosuppression by mesenchymal stem cells promoting the growth of prostate cancer cells. *Molecular Medicine Reports, 6*(5), 955–960. https://doi.org/10.3892/mmr.2012.1019
64. Montesinos, J. J., Mora-García, M. de L., Mayani, H., Flores-Figueroa, E., García-Rocha, R., Fajardo-Orduña, G. R., … Monroy-García, A. (2013). In vitro evidence of the presence of mesenchymal stromal cells in cervical cancer and their role in protecting cancer cells from cytotoxic T cell activity. *Stem Cells and Development, 22*(18), 2508–2519. https://doi.org/10.1089/scd.2013.0084
65. Abumaree, M. H., Al Jumah, M. A., Kalionis, B., Jawdat, D., Al Khaldi, A., Abomaray, F. M., … Knawy, B. A. (2013). Human placental mesenchymal stem cells (pMSCs) play a role as immune suppressive cells by shifting macrophage differentiation from inflammatory M1 to anti-inflammatory M2 macrophages. *Stem Cell Reviews and Reports, 9*(5), 620–641. https://doi.org/10.1007/s12015-013-9455-2
66. Shi, Y., Du, L., Lin, L., & Wang, Y. (2017). Tumour-associated mesenchymal stem/stromal cells: Emerging therapeutic targets. *Nature Reviews. Drug Discovery, 16*(1), 35–52. https://doi.org/10.1038/nrd.2016.193
67. Brandenburg, S., Turkowski, K., Mueller, A., Radev, Y. T., Seidlitz, S., & Vajkoczy, P. (2017). Myeloid cells expressing high level of CD45 are associated with a distinct activated phenotype in glioma. *Immunologic Research, 65*(3), 757–768. https://doi.org/10.1007/s12026-017-8915-1